Novel modal interferometer based on ring-core photonic crystal fiber

Weiguo Chen (陈卫国), Shuqin Lou (娄淑琴)*, Liwen Wang (王立文), and Shuisheng Jian (简水生)

Institute of Lightwave Technology, Key Lab of All Optical Network and Advanced Telecommunication Network, Ministry of Education, Beijing Jiaotong University, Beijing 100044, China

**E-mail: shqlou@bjtu.edu.cn*

Received May 12, 2010

An original design of ring-core photonic crystal fiber (RPCF) is proposed. By splicing a section of the homemade RPCF between two segments of single mode fibers (SMFs), a simple modal interferometer is presented and experimentally demonstrated. Owing to the effects of the collapsed region, the ring modes in RPCF can be effectively activated. To our knowledge, it is the first time to demonstrate the modal interferometer based on the interference between the ring modes, which is different from the previously reported interferometers based on the interference between core modes or cladding modes. The temperature and strain characteristics of the interferometers with different lengths of RPCF are investigated.

OCIS codes: 060.5295, 120.3180, 060.2370.

doi: 10.3788/COL20100810.0986.

Photonic crystal fibers (PCFs) have been widely studied owing to their unique properties such as single mode operation, large mode area, high birefringence, and so on[1−3]. Due to these flexible properties, PCFs offer the possibility to develop novel fiber interferometers for various applications. Some authors have demonstrated PCF interferometers for fiber sensors and wavelength-selective filters[4−7]. PCFs can be fabricated with pure silica which has low thermal expansion coefficient and low thermo-optic coefficient. Therefore, the PCF interferometers with temperature insensitivity have great advantages in fiber sensing. Frazão *et al.* reported a Sagnac loop interferometer with low temperature sensitivity for strain sensing[4]. Dong *et al.* presented a temperature-insensitive modal interferometer by finely core-offsetting a splice between the polarization maintaining PCF and single mode fiber (SMF)[5]. Jha *et al.* reported a simple modal interferometer for application in refractometry with the large-mode-area PCF[6]. Chen *et al.* proposed a switchable multi-wavelength fiber laser by using the PCF interferometer as the wavelength-selective filter[7].

In this letter, an original design of ring-core photonic crystal fiber (RPCF) is proposed. By splicing a section of the novel homemade RPCF between two segments of SMFs (Corning SMF-28), a simple modal interferometer is presented and experimentally demonstrated. The temperature and strain characteristics of the interferometers with different lengths of RPCF are investigated. The experimental results demonstrate that the interferometer can be used as a strain sensor with very low temperature sensitivity.

As shown in Fig. 1(a), the homemade RPCF is pure-silica PCF in which the arrays of air holes run along the fiber's length. The air holes in the cladding are arranged in a triangular lattice and the ring core of RPCF is formed by omitting the air holes in the third ring. The outer diameter of RPCF is 154 μm, the average diameter of the air holes is 5.49 μm, and the average hole pitch is 8.14 μm. The schematic diagram of the modal interferometer and the micrograph of the first collapsed region between SMF-in and RPCF are also shown in Fig. 1(a). Since the volume average refractive index of ring core is higher than that of the other regions in RPCF, the light can be guided through the ring core by a modified form of total internal reflection. The modes which can propagate steadily in the ring core of RPCF are called the ring modes[8]. According to the structure parameters of the homemade RPCF, it is the multi-mode RPCF that supports the low- and the high-order ring modes in the ring core. Several modal field distributions of the actual RPCF are depicted in Fig. 1(b). Compared with the conventional fiber, the ring core of RPCF is closer to the external environment. Therefore, the modal interferometer based on RPCF may be sensitive to the external disturbance and can be suitable for the measurement of strain and microbend, etc.

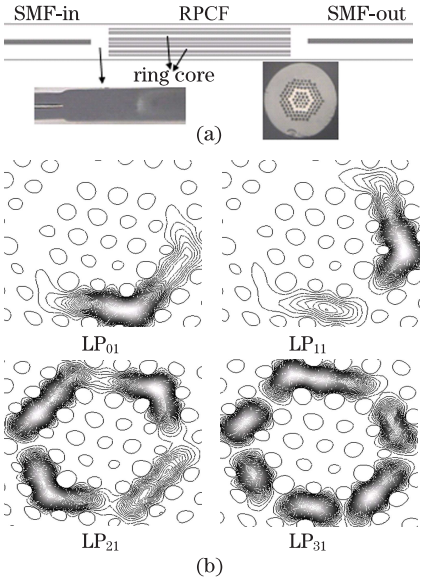

Fig. 1. (a) Micrograph of the cross section of the homemade RPCF, schematic diagram of the modal interferometer, and micrograph of the first collapsed region; (b) several modal field distributions of the actual RPCF.

 © 2010 Chinese Optics Letters

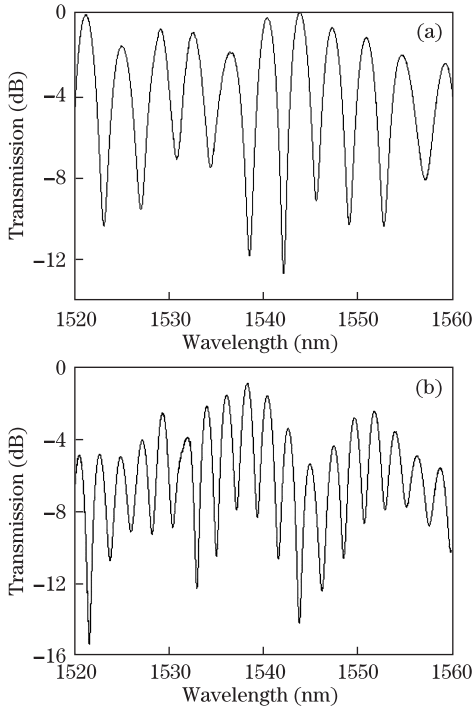

Fig. 2. Normalized transmission spectra of Interferometer (a) I and (b) II.

When SMF and RPCF are fusion spliced using a commercial fusion splicer (Ericsson FSU 975), there are a fully collapsed region at the beginning of the splice region and a tapered transition region between SMF and RPCF. The tapered region is the zone where the air holes of RPCF are tapered. By placing two splice regions between SMF and RPCF, a simple modal interferometer is constructed. The splices are high strength and permanent, and thus the long-term reliability of the interferometer is ensured.

When the fundamental mode in SMF propagates into the RPCF through the first collapsed region, the solid region of pure silica (i.e., the first fully collapsed region) makes the fundamental mode from SMF spread out. Part of the power can be coupled into the ring core of RPCF through the tapered region, and then activate the ring modes are activated. The excited low- and high-order ring modes propagate at different phase velocities along the section of RPCF, and thus the phase difference can be accumulated. When these excited modes converge in the second collapsed region, the modal interferences among the different modes which satisfy the interference condition will occur. The low- and high-order modes involved in the interference belong to the ring modes. Considering only the two main interfering modes, the interference fringe spacing is described by $P=\lambda^2/\Delta n_{\rm e}L$[6], where λ is the light wavelength, $\Delta n_{\rm e}$ is the effective refractive index difference between the interfering modes, and L is the length of RPCF.

Two interferometers were fabricated with RPCFs of 84.7- and 143.4-mm lengths. Here, the former is defined as Interferometer I, and the latter as Interferometer II. For Interferometer I, the lengths of the tapered regions and the fully collapsed regions are about 100 and 350 μm, respectively; for Interferometer II, these lengths are about 130 and 380 μm, respectively. The normalized transmission spectra of the two interferometers are shown in Fig. 2. It can be seen that the interferometer with longer length of RPCF has a narrower fringe spacing. Due to the existence of the collapsed regions, the insertion loss of the interferometers is about 9 dB. When the interferometer is used as the fiber sensor by monitoring the wavelength shift of the interference fringe, the loss is not an important factor affecting the measurement accuracy[5]. Furthermore, the loss can be further reduced by optimizing the fusion parameters, tapering, and adjusting the ring-core structure parameters such as the size and location of the ring core.

In order to analyze the number and energy distribution of the involved interfering ring modes, the corresponding spatial frequency spectra of the interferometers were calculated through the fast Fourier transform (FFT) method[9]. There are several peaks appearing in each spatial frequency spectrum, but there is only one dominant peak. That is to say, although more than two ring modes are excited in the proposed interferometer, there are only two main ring modes that predominate the modal interferences and form the main interference fringe. The interferences with other ring modes will form the modulation for the main interference fringe and make the ultimate interference fringe quasi-sinusoidally modulated. Besides, the air holes of RPCF are tapered with random orientation in the tapered regions. The introduced random parasitic birefringence and the polarization dependent loss also have effects on the interference fringe. The first collapsed region plays an important role in determining the number of the excited ring modes and the coupling strength of these modes[9]. Due to the difference of the lengths of the first collapsed region, the two interferometers have different side-lobes in the spatial frequency spectra which are formed by interferences of the different weak ring modes. In order to weaken the modulation effects of the weak ring modes on the interference fringe and get a uniform interference fringe, the length of the first collapsed region should be optimized by adjusting the fusion parameters. Further research is in progress.

When the strain or temperature change is applied to the interferometer, its transmission spectrum will have a wavelength shift. Because the RPCF is fabricated with pure silica, insensitivity to temperature is ensured. The proposed interferometer has advantages of its simple structure, high stability, low cost, and temperature insensitivity. Therefore, the interferometer can be used in strain sensing. The coating of RPCF was stripped off. An unpolarized amplified spontaneous emission (ASE) source was used as the light source. The transmission spectra were monitored by an optical spectrum analyzer (OSA, ANDO AQ6317) with a resolution of 0.01 nm. Figure 3 shows the wavelength shifts of the troughs around 1549 nm of the interferometers with the variations of temperature and strain. The insets are the transmission spectra of the interferometers under different temperatures and strains. Although the extinction ratio of the interferometers has slight fluctuations with the variations of strain or temperature, the interference fringes are still well maintained.

We measured the temperature sensitivity of the interferometers by placing them into a temperature-heating oven. The transmission spectra had a red shift with

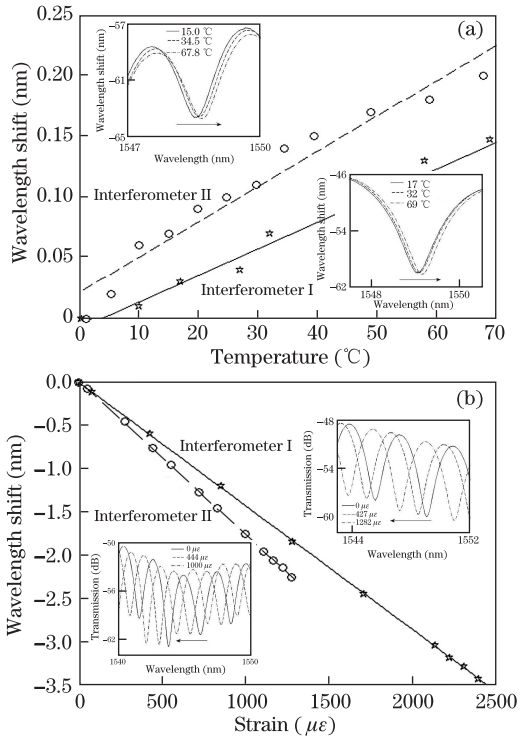

Fig. 3. Wavelength shift as a function of (a) temperature and (b) strain. The insets are the transmission spectra of the interferometers under different temperatures and strains. Circles and pentagrams are measured wavelength shifts of the troughs; lines are linear fitting to the measured data.

an increase of temperature over the range from 0 to 70 °C. The temperature sensitivity of Interferometer I is 2.2 pm/°C at 1549.04 nm, while that of Interferometer II is 2.91 pm/°C at 1548.5 nm. It can be seen that the interferometer with shorter length of RPCF has smaller temperature sensitivity. Such a sensitivity is much lower than that of Bragg gratings, long period gratings, or other interferometers based on PCF[6,10−12]. The wavelength shifts with respect to the strains of the interferometers were also measured by placing them on a linear mechanical transition stage at room temperature (13.5 °C). When the strain was gradually increased, the transmission spectra had a blue shift. By measuring the wavelength shift against the strain, a good linear relationship between the wavelength shift and the strain is obtained, as shown in Fig. 3(b). To keep the wavelength shift smaller than the fringe spacing, the interferometer with longer length of RPCF has a smaller measurement range. The strain sensitivity of Interferometer I is 1.434 pm/$\mu\varepsilon$, the coefficient of determination R^2 is about 0.9998, and the strain resolution is 6.97 $\mu\varepsilon$. For Interferometer II, the strain sensitivity is 1.777 pm/$\mu\varepsilon$, R^2 is over 0.9998, and the strain resolution is about 5.62 $\mu\varepsilon$, respectively.

According to the above analysis, the interferometer with longer length of RPCF has narrower fringe spacing, larger strain sensitivity, and higher strain resolution, but it has a smaller strain measurement range. The RPCF is fabricated with pure silica, therefore the low temperature sensitivity of the modal interferometer is ensured. The fiber strain sensor is usually operated in the normal environment in which the temperature has a slight fluctuation. Due to the low temperature sensitivity of the interferometer, it can be operated for strain measurement in normal environment with a slight temperature fluctuation. It is demonstrated that the interferometer, which has a good strain sensitivity of 1.777 pm/$\mu\varepsilon$, is suitable for the use as a strain sensor with low temperature sensitivity.

In conclusion, a novel RPCF is proposed and fabricated with pure silica. By splicing a section of the novel homemade RPCF and two segments of SMFs, a simple modal interferometer is presented and experimentally demonstrated. Owing to the effects of the collapsed region, the ring modes in RPCF can be effectively activated. To our knowledge, it is the first time to demonstrate the interferometer based on the interference between the ring modes. The effects of the length of RPCF on the temperature and strain characteristics of the interferometer are investigated. The interferometer has very low temperature sensitivity. The interferometer with longer length of RPCF has larger strain sensitivity. The interferometer can be used as a strain sensor with low temperature sensitivity. Besides, the interferometer can also be used for refractive index sensing or evanescent wave chemical sensing. And the method to excite the ring modes in the fiber by collapsing air holes of RPCF has potential applications in mode converter and the generation of hollow beams.

This work was supported by the National Natural Science Foundation of China (No. 60977033), the Major State Basic Research Development Program of China (No. 2010CB328206), the Innovation Foundation for Excellent Doctorial Candidates of Beijing Jiaotong University (Nos. 141055522 and 141060522), and the Fundamental Research Funds for the Central Universities (Nos. 2009YJS004 and 2009YJS008).

References

1. P. St. J. Russell, J. Lightwave Technol. **24,** 4729 (2006).
2. Z. Wang, L. Zhang, J. Wang, and K. Yu, Acta Opt. Sin. (in Chinese) **29,** 2909 (2009).
3. M. Hu, Y. Song, B. Liu, X. Fang, C. Zhang, H. Liu, F. Liu, C. Wang, L. Chai, Q. Xing, and Q. Wang, Chinese J. Lasers (in Chinese) **36,** 1660 (2009).
4. O. Frazão, J. M. Baptista, and J. L. Santos, IEEE Sensors J. **7,** 1453 (2007).
5. B. Dong, D.-P. Zhou, and L. Wei, J. Lightwave Technol. **28,** 1011 (2010).
6. R. Jha, J. Villatoro, G. Badenes, and V. Pruneri, Opt. Lett. **34,** 617 (2009).
7. W. G. Chen, S. Q. Lou, S. C. Feng, L. W. Wang, H. L. Li, T. Y. Guo, and S. S. Jian, Laser Phys. **19,** 2115 (2009).
8. K. Oh, S. Choi, Y. Jung, and J. W. Lee, J. Lightwave Technol. **23,** 524 (2005).
9. L. V. Nguyen, D. Hwang, S. Moon, D. S. Moon, and Y. Chung, Opt. Express **16,** 11369 (2008).
10. J. Villatoro, V. Finazzi, V. P. Minkovich, V. Pruneri, and G. Badenes, Appl. Phys. Lett. **91,** 091109 (2007).
11. C. Martelli, J. Canning, N. Groothoff, and K. Lyytikainen, Opt. Lett. **30,** 1785 (2005).
12. Y.-P. Wang, L. Xiao, D. N. Wang, and W. Jin, Opt. Lett. **31,** 3414 (2006).